

## **General Disclaimer**

### **One or more of the Following Statements may affect this Document**

- This document has been reproduced from the best copy furnished by the organizational source. It is being released in the interest of making available as much information as possible.
- This document may contain data, which exceeds the sheet parameters. It was furnished in this condition by the organizational source and is the best copy available.
- This document may contain tone-on-tone or color graphs, charts and/or pictures, which have been reproduced in black and white.
- This document is paginated as submitted by the original source.
- Portions of this document are not fully legible due to the historical nature of some of the material. However, it is the best reproduction available from the original submission.

DETERMINATION OF LAUNCH CONDITIONS FOR SPACELAB SATISFYING THE  
CONSTRAINTS OF AN ABSORPTION SPECTROSCOPY PROJECT

J. Vercheval

(NASA-TM-75465) DETERMINATION OF LAUNCH  
CONDITIONS FOR SPACELAB SATISFYING THE  
CONSTRAINTS OF AN ABSORPTION SPECTROSCOPY  
PROJECT (National Aeronautics and Space  
Administration) 16 p HC A02/MF A01 CSCL 22A G3/12

N79-16885

Unclas  
13762

Translation of "Détermination des conditions de lancement de  
Spacelab en vue de satisfaire les exigences d'un projet  
d'expérience par spectrométrie d'absorption," European Space  
Agency Journal, Vol. 2, No. 1, 1978, pp. 19-26.



# DETERMINATION OF LAUNCH CONDITIONS FOR SPACELAB SATISFYING THE CONSTRAINTS OF AN ABSORPTION SPECTROSCOPY PROJECT

J. Vercheval  
ESA

## Introduction

Within the framework of the Spacelab program, the Belgian <sup>\*/20</sup> Space Aeronomy Institute in cooperation with the National Office for Aerospace Studies and Research (ONERA, France) developed an experimental project using the technique of absorption spectroscopy: the instrument chosen, in this case a grating spectrometer, is to measure the absorption of solar radiation by various minor constituents of the homosphere in the infrared region of the spectrum between 2 and 13  $\mu\text{m}$ . Absorption spectrometry is a fundamental method for studying the constituents of the atmosphere. It has been used quite frequently in observations made from the earth or from aircraft or stratospheric balloons. But these various special observation conditions present a series of very strict limitations in time as well as according to the three dimensions of space. These limitations are mainly due to meteorological constraints and to the limited number of observation stations. On the other hand, coverage in time and in space may prove to be much greater if the same technique is used from a space vehicle such as Spacelab.

During its first mission, Spacelab is to remain in orbit for seven days. Under these conditions, the coverage of observations in space will depend on the characteristics of

---

\* Numbers in the margin indicate pagination in the foreign text.

the chosen orbit, the launching time and the time of the year. The results presented in this report only deal with latitude coverage.

### Definition of the Problem

The geometrical aspects of the problem presented will be treated by assuming that the sun is a point and the earth a sphere of radius  $R_1$  equal to 6370 km. However, it should be specified that in calculating the movement of Spacelab, the precession of the orbit due to the flattening of the earth at the poles will be taken into account.

In fact, the proposed experiment will consist of pointing the sun close to the limb of the earth, the atmospheric region to be observed extending from 20 to 100 km in altitude. Consequently, 20 and 100 are the lower and upper limits between which the solar radiation must graze the earth sphere before being received by the spectrometer. With each revolution involving an occultation of Spacelab, these special observation conditions will occur during the few moments preceding or following occultation. In the first place, it involves knowing the duration of the observations, which requires the determination of the moments  $t(20)$  (or  $t'(20)$ ) and  $t(100)$  (or  $t'(100)$ ) at which the levels 20 and 100 are reached by the solar radiation before occultation (or after occultation). This boils down to a properly so-called problem of occultation when the radius of the earth is imaginarily increased by 20 and 100 km respectively.

The latitude and longitude coverage of the observations is also important to know. Thus there is the problem of calculating the geographical coordinates of the tangential points of solar radiation with the level limitations.

The attitude of Spacelab in relation to a system of axes linked to its center of mass, is an essential factor in the problem. Once the attitude is determined, one must be sure, for example,

that the empennage of the aircraft is not obstructing the path of the solar radiation during the periods which are theoretically favorable for observation. That is why it is also necessary to know the pointing angles assigned to the system of axes adopted.

### Calculation Method

#### Determining Equatorial Passages

We assume that Spacelab was launched on day J at  $t_0$  time (universal time) from the Cape Kennedy base. Assuming that passage to the ascending node N marks the beginning of each new /21 revolution, we can agree upon the theory that the first revolution is begun at the moment  $t_{N.1}$ , a few minutes before time  $t_0$ . Time  $t_{N.1}$  and the corresponding west longitude  $\lambda_{N.1}$  are determined in such a way that the application of the laws of elliptical movement ensure passage above Cape Kennedy at time  $t_0$ . By continuing in this manner, the power phase of the launching is disregarded. The reservations implied by this approximation, as to the results obtained, cannot be serious, if not less than those attributable to the inevitable inaccuracies involved in placing a vehicle into orbit. The parameters  $t_{N.1}$  and  $\lambda_{N.1}$  being known, we deduce the straight ascension of the ascending node  $\Omega_1$  by the relation:

$$\Omega_1 = \alpha_0 + t_{N.1} - \lambda_{N.1} + E - 12h \quad (1)$$

where  $\alpha_0$  and E designate the straight ascension of the sun and the equation of the time on day J at time  $t_{N.1}$  respectively. For any revolution r, we have:

$$t_{N,r} = t_{N.1} + (r-1)P \quad (2)$$

$$\lambda_{N,r} = \lambda_{N.1} + \Delta\lambda_N(r-1) \quad (3)$$

$$\Omega_r = \Omega_1 + \Delta\Omega(r-1) \quad (4)$$

P designates the revolution period of Spacelab (89.3 mn).

$\Delta\lambda_N$  is a coefficient representing the variation in the longitude of the ascending node during one revolution. This variation



results from the rotation of the earth sphere around its axis and from the precession movement of the orbit; thus,  $\Delta z_N$  is given by the relation:

$$\Delta z_N = 0.25068P + \frac{10}{n} \left( \frac{R_E}{a} \right)^{3.5} \cos i \quad (5)$$

where the coefficient 0.25068 is the angle of rotation (expressed in degrees) of the earth sphere in one minute, the period P itself is expressed in minutes; n is the average movement, i and a designate the inclination and the geocentric radius of the orbit respectively;  $R_E$  is the equatorial radius of the earth sphere.

The coefficient  $\Delta \Omega$  designates the variation in  $\Omega$  during one revolution; its expression is given by the second term, with the sign changed, of the right-hand side of the formula (5).

#### Determining Periods Favorable for Observation

The general problem to be solved is that of determining the times  $t_1(z)$  and  $t_r'(z)$ , during any revolution r, at which the "observed" solar radiation passes at the altitude level z. Later on, we will drop the r in order to alleviate the writing. As we have already mentioned, this problem may be boiled down to a problem of occultation if a fictitious earth of radius  $R = R_T + z$  ( $R_T = 6370$  km) is adopted. In a first stage, we agree that during one revolution, the sun and the orbital plane remained fixed in relation to a system of non-rotating geocentric axes.

Let u be the geocentric angle between the ascending node N and the space vehicle S, measured from the node in the direction of movement (Fig. 1). During each revolution r, the points of the orbit marking the beginning and the end of occultation are determined by particular values of this angle. The latter, in the cases of u and u' are obtained from the relation<sup>1</sup>:

$$\cos(u - \theta) = \cos(u' - \theta) = - \frac{R}{a \sin \eta} \sqrt{\frac{a^2}{R^2} - 1} \quad (6)$$

$\eta$  is the angle created by the radius vector Earth-Sun OA with the line OK perpendicular to the orbital plane pointed in the 22

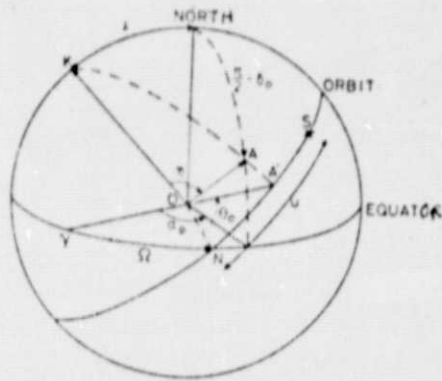


Figure 1. Representation of Angles  $\eta$  and  $O_{\odot}$ .

- O Center of the Earth
- A Sun
- S Spacelab
- N Ascending Node
- Y First Point of Aries or Vernal Equinox

direction of angular momentum.  $O_{\odot}$  is the geocentric angle between the ascending node N and the orthogonal projection OA of radius OA in the orbital plane.

Due to symmetry, angles  $(u - O_{\odot})$  and  $(u' - O_{\odot})$  belonging to the second and third quadrants are related in the following way:

$$(u - O_{\odot}) = 360^{\circ} - (u' - O_{\odot}) \quad (7)$$

Angles  $\eta$  and  $O_{\odot}$  are calculated by applying the classical

formulas of spherical trigonometry:

$$\cos \eta = \cos i \sin \delta_{\odot} - \sin i \cos \delta_{\odot} \sin (z_0 - \Omega) \quad (8)$$

$$\cos O_{\odot} = \frac{\cos (z_0 - \Omega) \cos \delta_{\odot}}{\sin \eta} \quad (9)$$

where  $O_{\odot}$  is the declination of the sun. The parameters  $\alpha_{\odot}$ ,  $\delta_{\odot}$ , and  $\Omega$  are evaluated at time  $t_N$  of passage to the ascending node from the revolution considered.

For  $\cos O_{\odot} > 0$ ,  $O_{\odot}$  belongs to the first quadrant if the condition  $-\arcsin(\operatorname{tg} i \operatorname{tg} \delta_{\odot}) < z_0 - \Omega < 90^{\circ}$  is satisfied,  $\arcsin(\operatorname{tg} i \operatorname{tg} \delta_{\odot})$  always being taken in the first quadrant.

For  $\cos O_{\odot} < 0$ ,  $O_{\odot}$  belongs to the second quadrant if the condition  $90^{\circ} < z_0 - \Omega < 180^{\circ} + \arcsin(\operatorname{tg} i \operatorname{tg} \delta_{\odot})$  is verified.

The times  $t(z)$  and  $t'(z)$ , previously defined, can be deduced from the information about angles  $u$  and  $u'$ . We have

$$\left. \begin{aligned} t(z) &= t_N + \frac{u}{360} P \\ t'(z) &= t_N + \frac{u'}{360} P \end{aligned} \right\} \quad (10)$$

The angles  $u$  and  $u'$  expressed in degrees are calculated with the

values of the parameters  $\alpha_0$ ,  $\delta_0$  and  $\Omega$  at time  $t_N$ . These values are maintained during the revolution. However, afterwards, certain angles are determined at times  $t(z)$  and  $t'(z)$  which involve a very precise knowledge of the positions of the sun, the orbit, and Spacelab. In particular, the time (based on the position of the sun) as well as the parameters determining these positions must constitute a coherent system. That is why the formulae developed above are once again applied with the values of the parameters  $\alpha_0$ ,  $\delta_0$  and  $\Omega$  relating to the times  $t(z)$  and  $t'(z)$  successively. The new values obtained for  $u$ ,  $u'$ ,  $t(z)$  and  $t'(z)$  are considered to be definitive. The distances in the first results are measured in tenths of a degree and tenths of a minute (time) and need not be repeated.

#### Determination of Coverage of the Observations

Let  $T$  and  $T'$  be tangential points of the solar radiation with level  $(z)$  relative to time  $t(z)$  and  $t'(z)$  respectively. In Figure 2, we have depicted on the unitary sphere the relative positions of the sun (A), Spacelab (S), and a tangential point (T).

Let  $(\phi_s, \lambda_s)$  and  $(\phi_t, \lambda_t)$  be the western latitudes and longitudes of points S and T. The following relations can be easily deduced:

$$\sin \phi_t = \frac{\sin \phi_s + \sin D \sin \delta}{\cos D} \quad (11)$$

$$\lambda_t = \lambda_s \pm \arccos \left( \frac{\cos D - \sin \phi_s \sin \phi_t}{\cos \phi_s \cos \phi_t} \right) \quad (12)$$

where  $D$  designates the local solar depression at point S; when 23 the altitude  $z$  of the tangential point is fixed, the solar depression is a constant whose value is obtained by applying the formula

$$D = \arccos \left( \frac{R_1 + z}{a} \right) \quad (13)$$



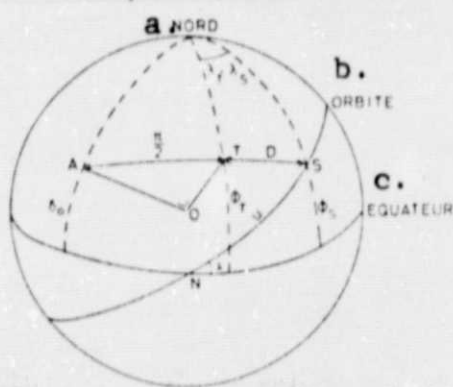


Figure 2. Representation of the Relative Positions of Spacelab (S), the Sun (A), and the Tangential Point (T). a. North, b. Orbit, c. Equator

The signs + or - are adopted depending on whether the difference in longitudes between the sun and Spacelab ( $\lambda_S - \lambda_A$ ) is less than or greater than  $180^\circ$ .

The determination of  $\phi_T$  and  $\lambda_T$  implies a previous knowledge of the latitude  $\phi_S$  and the longitude  $\lambda_S$ . These elements are given by the relations

$$\sin \phi_S = \sin i \sin u \quad (14)$$

$$\lambda_S = \lambda_N - \arcsin(\cotg i \tg \phi_S) + \left[ 0.25068 + \frac{1}{144} \left( \frac{R_t}{a} \right)^{3.5} \cos i \right] [t(z) - t_N] \quad (15)$$

where the second term of the right-hand side of the equation takes the longitudinal movement of Spacelab into consideration. The third and fourth terms represent the contributions due to the rotation of the earth sphere and to the precession of the orbit respectively. The time difference is expressed in minutes.

Knowledge of the geographical coordinates of points T and T' for each revolution allows the coverage of the operations to be specified.

#### Determination of the Pointing Angles

Suppose there is a system of axes (S,x,y,z) located at the center of mass S of Spacelab (Fig. 3). The axes Sx and Sz are located in the orbital plane pointed in the direction of the speed vector v and the geocentric radius vector OS respectively. The axis Sy is perpendicular to the orbital plane and pointed in the direction of the angular momentum vector. The direction of the sun in relation to this set of axes can be defined by two

pointing angles: on the one hand, the bearing angle  $G$  measured in the local horizontal plane ( $Sx$ ,  $Sy$ ) and measured from the axis  $Sx$  positively towards axis  $Sy$ , and, on the other hand, the elevation angle  $H$  measured from the horizontal plane positively towards axis  $Sz$ . Suppose there is a second system of axes ( $O, X, Y, Z$ ) located at the center of the earth; axes  $OX$  and  $OY$  are located in the equatorial plane, axis  $OX$  pointed towards the first point of Aries. Axis  $OZ$  is pointed towards the North Pole.

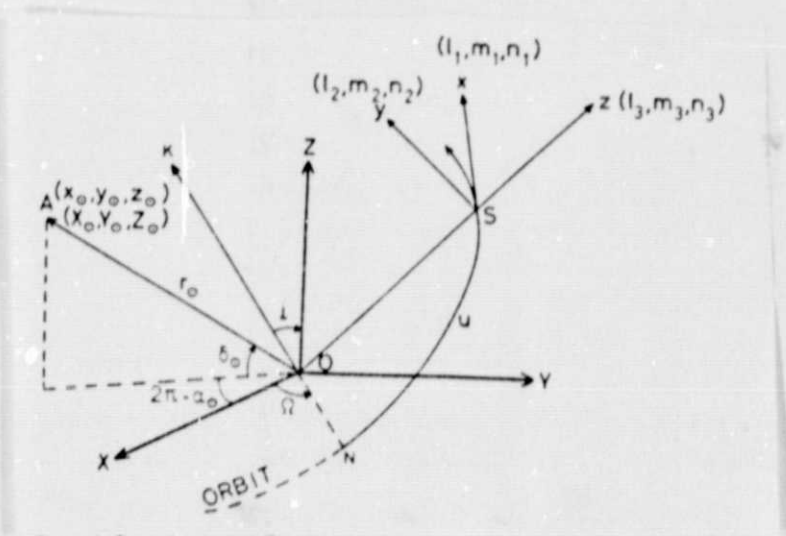


Figure 3. Representation of the Systems of Axes ( $O, X, Y, Z$ ) Which Join at the Center of the Earth  $O$  and ( $S, x, y, z$ ) Which Join at the Center of Mass  $S$  of Spacelab

Angles  $G$  and  $H$  /24 are determined while considering the radius of Spacelab's orbit in relation to the distance Earth-Sun  $r_0$  to be negligible, which leads us to agree that the two systems of axes have the same origin in the transformation formulas of the coordinates of any system of axes. If  $(l_1, m_1, n_1)$ ,  $(l_2, m_2, n_2)$  designate the direction cosines of axes  $Sx$ ,  $Sy$

and  $Sz$  respectively with respect to axes  $OX$ ,  $OY$  and  $OZ$ , we can write the following relations:

$$\left. \begin{aligned} x_0 &= l_1 X_0 + m_1 Y_0 + n_1 Z_0 \\ y_0 &= l_2 X_0 + m_2 Y_0 + n_2 Z_0 \\ z_0 &= l_3 X_0 + m_3 Y_0 + n_3 Z_0 \end{aligned} \right\} \quad (16)$$

On the other hand, we have

$$\left. \begin{aligned} x_0 &= r_0 \cos H \cos G \\ y_0 &= r_0 \cos H \sin G \\ z_0 &= r_0 \sin H \end{aligned} \right\} \quad (17)$$

$$\left. \begin{aligned} X_0 &= r_0 \cos \alpha_0 \cos \delta_0 \\ Y_0 &= r_0 \sin \alpha_0 \cos \delta_0 \\ Z_0 &= r_0 \sin \delta_0 \end{aligned} \right\} \quad (18)$$

$$\left. \begin{aligned} l_1 &= -\cos \Omega \sin u - \sin \Omega \cos u \cos i \\ m_1 &= -\sin \Omega \sin u + \cos \Omega \cos u \cos i \\ n_1 &= \cos u \sin i \end{aligned} \right\} \quad (19)$$

$$\left. \begin{aligned} l_2 &= \sin \Omega \sin i \\ m_2 &= -\cos \Omega \sin i \\ n_2 &= \cos i \end{aligned} \right\} \quad (20)$$

$$\left. \begin{aligned} l_3 &= \cos \Omega \cos u - \sin \Omega \sin u \cos i \\ m_3 &= \sin \Omega \cos u + \cos \Omega \sin u \cos i \\ n_3 &= \sin u \sin i \end{aligned} \right\} \quad (21)$$

The combination of systems (16) through (21) leads to the following three formulas giving the angles H and G which we have been trying to find.

$$\begin{aligned} \sin H &= \cos \delta_0 \cos \alpha_0 (\cos \Omega \cos u - \sin \Omega \sin u \cos i) \\ &+ \cos \delta_0 \sin \alpha_0 (\sin \Omega \cos u + \cos \Omega \sin u \cos i) + \sin \delta_0 \sin u \sin i \end{aligned} \quad (22)$$

$$\begin{aligned} \cos G &= \frac{1}{\cos H} \left[ -\cos \delta_0 \cos \alpha_0 (\cos \Omega \sin u + \sin \Omega \cos u \cos i) + \cos \delta_0 \sin \alpha_0 \right. \\ &\left. (-\sin \Omega \sin u + \cos \Omega \cos u \cos i) + \sin \delta_0 \cos u \sin i \right] \end{aligned} \quad (23)$$

$$(24) \quad \underline{125}$$

It should be pointed out that angle H is the same as depression D with a different sign, whose expression (13) is absolute

although obviously more simple. A comparison of the results allows one to evaluate the precision of the method described, and especially, the coherence of the parameters which intervene. Lastly, when the attitude of Spacelab is specified after some time, as well as the position of the spectrometer on the vane, appropriate transformations will allow the definitive pointing angles  $H'$  and  $D'$  to be determined, this time referred to a reference system linked to Spacelab.

#### Latitude Coverage: Results

Latitude coverage of the observations is represented in Figures 4 through 6 with the hypothesis that the observations occur during 115 successive revolutions, or during approximately 7 days, at three particular times of the year: the vernal equinox and the June and December solstices. The launching time, expressed in universal time, another essential parameter in this problem, is reported according to the x-axes. The observations are referred to the altitude  $z$  of 20 km. Lastly, it should be pointed out that coverage of the observations made shortly before occultation (immersion) is marked by the broken line curves; the continuous line curves indicate the boundaries of the coverage of observations made shortly after occultation (emersion). The arrows indicate the direction of latitude variation during the 115 revolutions.

Figure 4 shows that during the vernal equinox, the most extensive coverage is ensured for the launching times close to 0 h 30, 3 h 30, 12 h 30 and 15 h 30: in the first two cases, the observations cover more of the northern hemisphere (0 to  $60^\circ$ ) than the southern hemisphere (0 to  $30^\circ$ ). The reverse occurs in the two other cases. Moreover, for launchings occurring at 2 h and 14 h, the same area of latitudes is scanned twice: 0 to  $50^\circ$  north (at 2 h) and 0 to  $50^\circ$  south (at 14 h). In actual fact, these conclusions are also valid for the September equinox. Coverage for a launching which occurred during the June solstice



is shown in Figure 5. It can be noted that for the launch times between 0 and 4 h, there is a 10 to 20 degree gap due, in fact, to periods of nonoccultation which appear under special launching conditions. Thus, for a launching set at 3 h 30, the phenomenon of occultation ceases after revolution No. 81. On the other hand, for a launching which occurred at 1 h 30, occultation does not occur until revolution No. 72. For launchings set between 1 h 30 and 2 h 30, /26 the periods of nonoccultation occur within the interval of seven days adopted as the duration for the experiment. Although there are gaps at periods of nonoccultation, coverage proves, nevertheless, to be greatest for launching times between 0 h and 4 h. It should be pointed out that it is also extensive for launchings made at 12h 30 and 15 h 30. Lastly, the same area of latitudes is scanned twice if the launch time is set at 2 h or 14 h. The preceding remarks also make the examination of Figure 6 relative to the December solstice necessary. Yet we notice a shift of 12 h between the launch times ensuring a coverage practically identical in amplitude. Furthermore, in December, the gap in coverage, due to periods of nonoccultation, is observed in the southern hemisphere.

Figure 7 shows, for the December solstice, the latitude variations of observations from one revolution to the next. Four launch times have been mentioned: 1 h 30, 3 h 30, 12 h and 15 h. The last two bring about a very extensive coverage of observations, one at the beginning of occultation, the other at the end of occultation. It seems that in these two cases, the observations are not equally distributed over latitude. Thus, for a launching made at 15 h, the latitude decreases from  $+36^{\circ}$  to  $+27^{\circ}$  during the first twenty revolutions, while it varies from  $+12^{\circ}$  to  $-27^{\circ}$  between revolutions No. 40 and 60. On the other hand, for launch times set at 1 h 30 and 3 h 30, the variation of latitude with time is linear. These findings may take on importance when launch conditions must



be chosen in terms of criteria set by the planned experiment.

### Conclusions

This work has demonstrated that the conditions for observing the homosphere by the absorption spectrometry technique performed from a space vehicle, depend very closely on the parameters setting the launching conditions, namely the time of year and the launch time. Since the latitude coverage is very sensitive to the launch time, it is especially important that the requirements which one hopes to meet within the framework of the planned experiment are well specified at the outset.

### Acknowledgments

I would like to thank Mr. Rosseeuw who took charge of the computer calculations program.

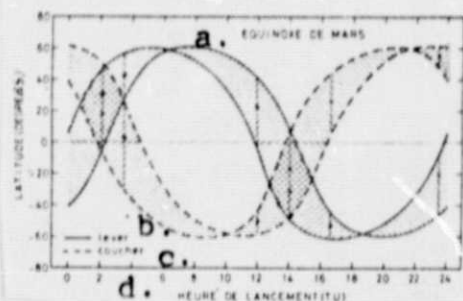


Figure 4. Latitude coverage of observations at 20 km altitude in terms of launch time and for the vernal equinox. The period of observations extends over 115 revolutions. The solid and broken line curves define the coverage boundaries at emersion and immersion (sun) respectively. The arrows indicate the direction of latitude variation. a. March equinox, b. Emersion, c. Immersion, d. Launch time.

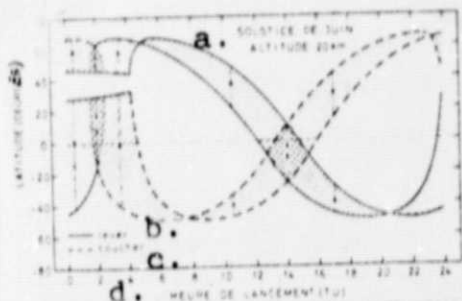


Figure 5. Latitude coverage for observations at 20 km altitude, as a function of launch time and for the June solstice.  
a. June solstice, b. Emer-sion, c. Immersion, d. Launch time.

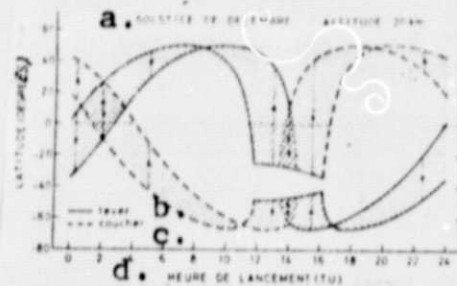


Figure 6. Latitude coverage for observations at 20 km altitude, as a function of launch time and for the December solstice.  
a. December solstice, b. Emer-sion, c. Immersion, d. Launch time.

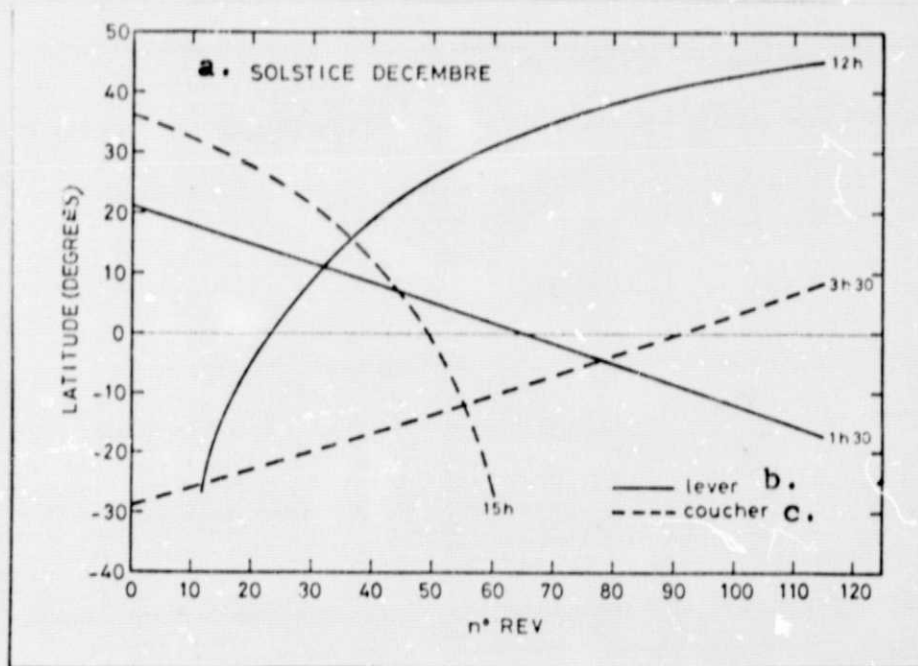


Figure 7. Latitude variations for observations at 20 km altitude, during the December solstice and for four different launch times (1 h 30, 3 h 30, 12 and 15 h).  
a. December solstice, b. Emer-sion, c. Immersion,